ITHERM 2019

IEEE ITherm Conference

The Intersociety Conference on Thermal and Thermomechanical Phenomena in Electronic Systems

Experimental Characterization of a Manifold-Microchannel Heat Exchanger Fabricated Based on Additive Manufacturing

William C. Yameen , Nathan A. Piascik, Riccardo C. Clemente , Andrew K. Miller
Seyed A. Niknam, Jingru Benner, Anthony D. Santamaria, Mehdi Mortazavi
Department of Mechanical Engineering, Western New England University, Springfield, MA 01119

WESTERN NEW ENGLAND UNIVERSITY College of Engineering

Background

- Power plants traditionally use water-cooled systems. Currently, over 98% of the thermoelectric power plants in the U.S. are cooled based on water-cooling systems. Such power plants consume 41% of freshwater in the U.S.
- Environmental water is used to cool down the steam in this cycle, which is returned to its environment after use at a much higher temperature. This creates a variety of ecological issues such as accelerated soil erosion, and adds geographic restrictions to power plants which need to be located near a source of freshwater.
- In contrast to this, air-cooled power plants require little or no water in their cooling systems. The experimental heat exchanger (HX) should still result in relatively low air-side pressure drop in order to avoid excess blower power. With an efficient enough design, air-cooled HXs could result in larger heat transfer rates compared to water-cooled HXs.
- Innovative HX designs can be constructed with additive manufacturing which is a powerful fabrication method using a technique known as Direct Metal Laser Sintering.
- Direct Metal Laser Sintering (DMLS) is an additive manufacturing process that uses a laser to sinter a thin layer of metallic dust that builds the part from the bottom up until the desired geometry is achieved. DMLS allowed for the most cost effective result, as well as provides dimensional accuracy and functionality.

Objective

In this study, heat transfer characteristics of a metallic air-water heat exchanger fabricated via additive manufacturing is investigated. In this type of heat exchangers, air is supplied into inlet manifolds from one side and exists the heat exchanger from outlet manifolds on the other side. Each air inlet manifold is blocked at the end while adjacent manifolds are open. Air passes from microchannels, fabricated on the top and bottom surfaces of the manifolds, to enter into adjacent manifolds. Water is supplied into water channels located underneath air microchannels.

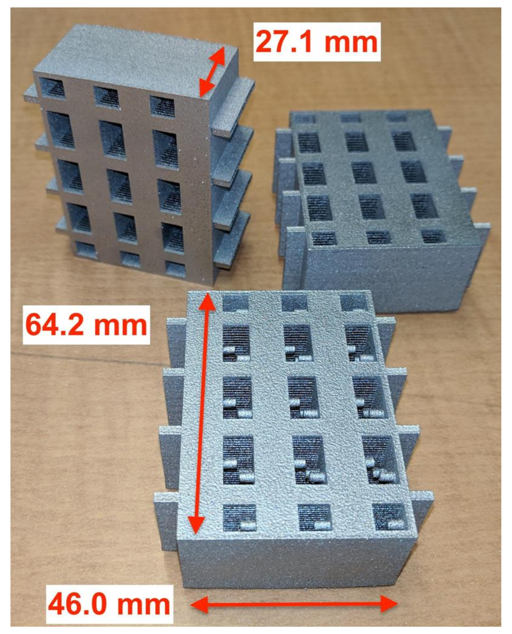

Water channel width	2.60 mm
Water channel height	1.10 mm
Air manifold width	6.42 mm
Air manifold height	11.24 mm
Microchannel fin height (H_{mc})	1.0 mm
Microchannel width (W_{mc})	0.48 mm
Thickness of microchannel fins	0.48 mm
Base thickness (L)	0.48 mm
Number of water channel rows	4
Number of water channels in each row	8
HX overall height (H_{HX})	64.20 mm
HX overall width (W_{HX})	46.02 mm
HX overall depth (D_{HX})	27.16 mm
Thickness of the heat exchanger body (T_{HX})	1.5 mm
Heat Exchanger Type A..........	without pin array (original)
Heat Exchanger Type B..........	with pin array
Heat Exchanger Type C..........	with pin array and modified microchannel orientation

Figure 1: Additively manufactured manifold-microchannel heat exchangers from stainless steel with dimensions.

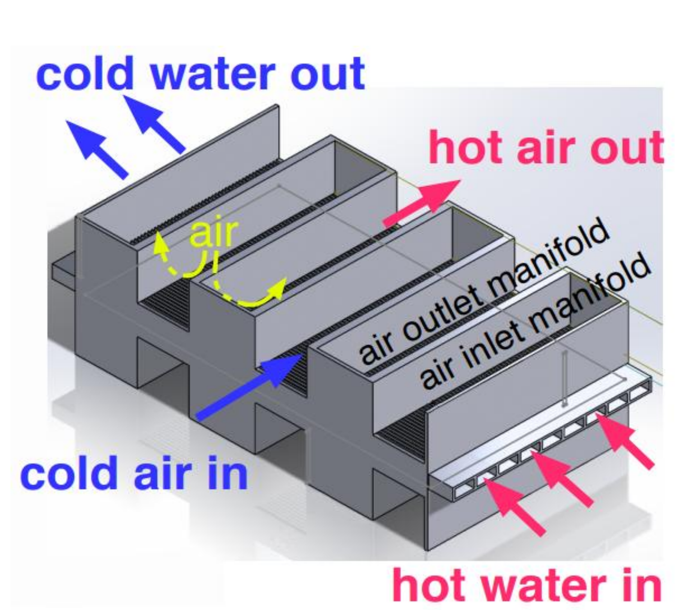

Figure 2: Single repeatable unit of manifold microchannel heat exchanger

Experimental Setup

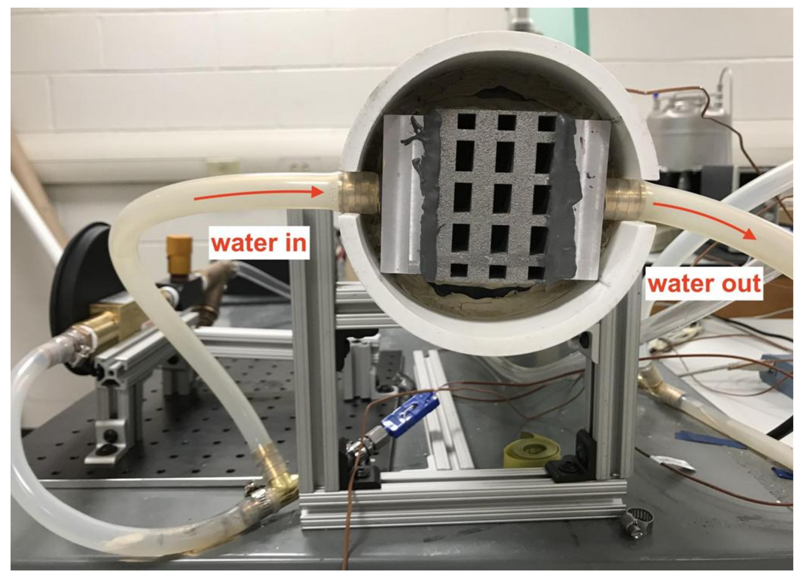

Figure 3: Mounted heat exchanger with water directions

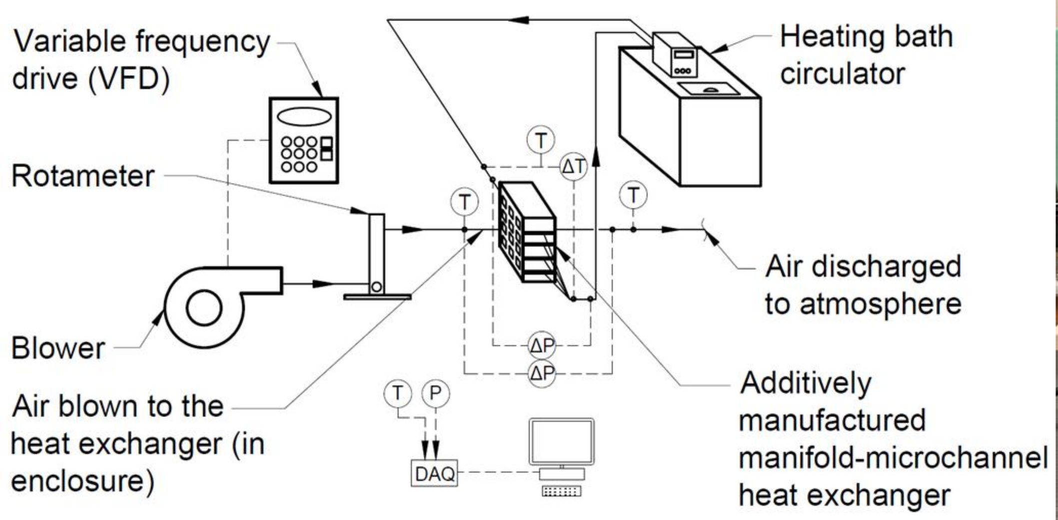

Figure 4: Experimental Setup Diagram

Figure 5: Experimental setup with air directions

- Tests conducted for each heat exchangers.
- Circulated water temperatures used were 50°C and 60°C.
- Air flow rate was measured at 6, 10, 15, 20, 25, and 30 ft³/min.
- Air flow was modulated via a VFD.
- Water flow rate was measured at 0.75 GPM which is equivalent to 0.047 l/s.
- Once blower was started, system ran for 20 minutes to reach steady state.
- PVC pipe was sealed behind the heat exchanger using plexiglass and a sealing agent.
- Uncertainty in temperature measurement was ±0.05°C, uncertainty in water flow was ± 0.0078 l/s, uncertainty in air flow was ± 0.24 l/s, and uncertainty in pressure measurement was ± 25 Pa.

Results and Discussion

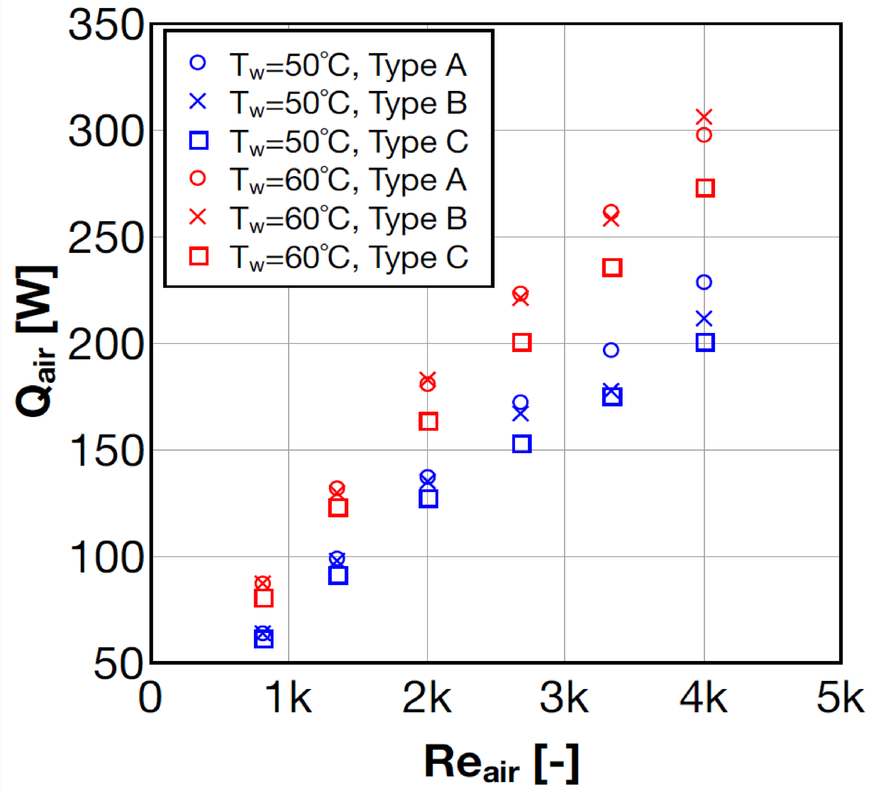

Figure 6: Air side heat flow rate calculated at different Reynolds number.

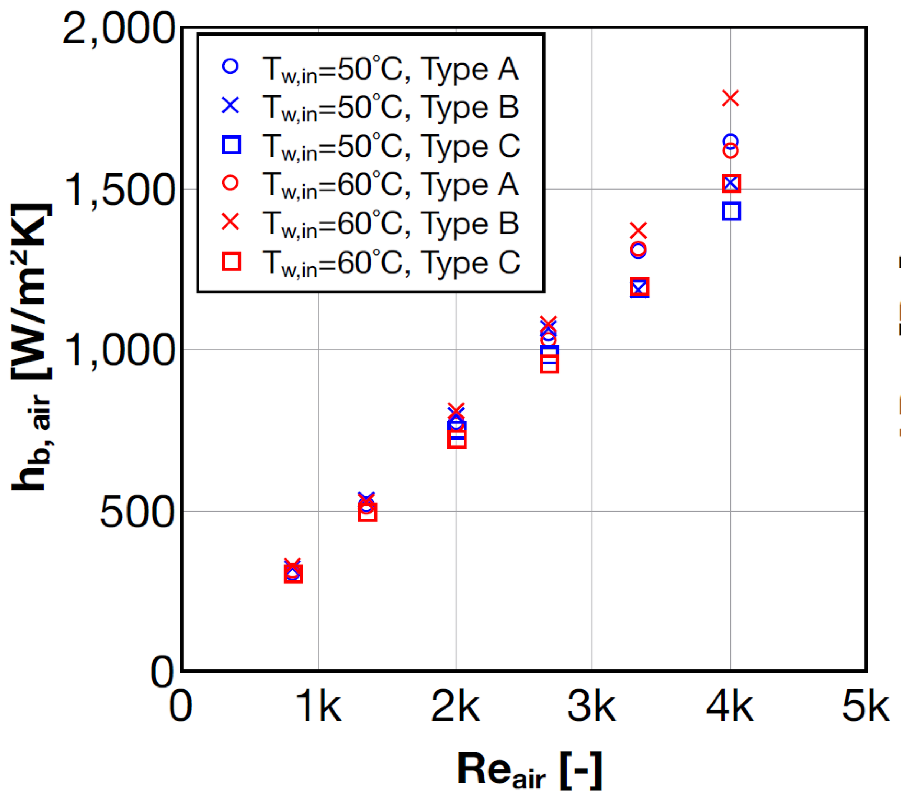

Figure 7: Air side convection heat transfer coefficient at different Reynolds number.

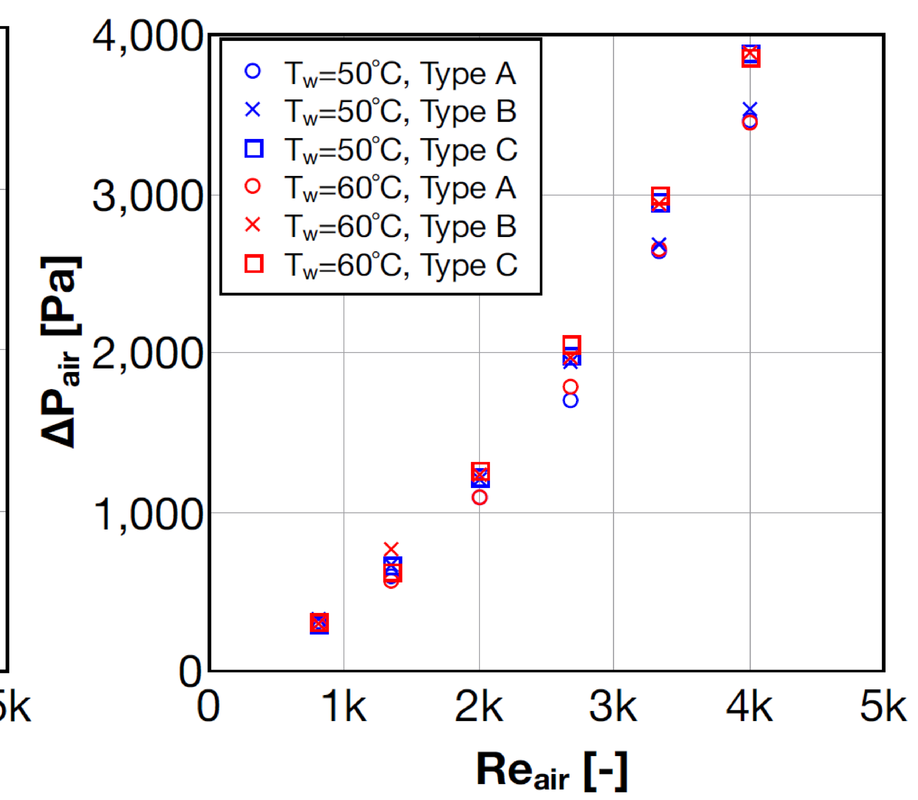

Figure 8: Air-side pressure drop for different air Reynolds numbers.

- Figure 6 shows the heat flow rate compared amongst the type A, B, and C heat exchangers in this study. The largest air-side heat flow for water inlet temperature of 50°C was around 228 W on the type A heat exchanger. For water inlet temperature of 60°C this number was 310 W on the type B heat exchanger.
- Figure 7 shows the air-side base convection heat transfer coefficient for different air Reynolds numbers tested in this study. The highest air side convection heat transfer coefficient for these heat exchangers was over 1,600 W/m²K for the type A heat exchanger at 50°C. The highest air side convection heat transfer coefficient obtained was over 1,750 W/m2K for the type B heat exchanger at 60°C.
- Figure 8 shows the pressure drop for the range of air flow rate tested in this study was between around 280 and 3,450 Pa for type A at both 50 and 60°C, between around 280 and 3750 Pa for type B at 50 and 60°C, and between around 280 and 3800 Pa for type C at 50 and 60°C.
- The equations used for these calculations can be seen below.

$$Q_{air} = \dot{m}_{air}\,_{air}\;(T_{air,out} - T_{air,out})$$

Equation 1: Q_{air} where m_{air}, $c_{p,air}$, $T_{air,in}$, and $T_{air,out}$ are air mass flow rate, air specific heat, air temperature in the inlet, and air temperature in the outlet of the heat exchanger, respectively.

$$h_{b,air} = \frac{Q_{air}}{A_{base}|T_{base} - T_{air,in}|}$$

Equation 2: $h_{b,air}$ where A_{base} and T_{base} are base surface area and base average temperature, respectively.

$$Re_{air} = \frac{\rho_{air} V D_h}{\mu_{air}}$$

Equation 3: Re_{air} where ρ_{air} ,and V are air density and velocity, respectively.

$$f = (0.790 ln Re_D - 1.64)^{-2}$$

Equation 4: f, the friction factor

$$Nu_D = \frac{\left(\frac{f}{8}\right)(Re_D - 1000)Pr}{1 + 12.7\left(\frac{f}{8}\right)^{\frac{1}{2}}\left(Pr^{\frac{2}{3}} - 1\right)}$$

Equation 5: Nu_D where Re_d, and Pr are Reynold's Number for a duct, and the Prandtl Number, respectively.

$$\frac{Nu_D}{Nu_{D,fd}} = 1 + \frac{C}{\left(\frac{x}{D}\right)^m}$$

Equation 6: The average Nusselt number for the entire water channel, where $C = 23.99Re^{-0.23}$ and $m = -2.08\times10^{-6}Re + 0.815$

$$D_h = \frac{4W_{mc}H_{mc}}{2W_{mc} + 2H_{mc}}$$

Equation 7 . D_h the hydraulic diameter

Conclusion

- Manifold-microchannel heat exchangers with slightly different interior designs were fabricated based on additive manufacturing techniques and from stainless steel
- Heat transfer characteristics of heat exchangers were evaluated at different air flow rates between 2.83 l/s and 14.16 l/s and different water temperatures. Water was supplied at 0.047 l/s.
- The highest air side heat transfer rates (Q_{air}) were obtained at 228 and 306 W for 50°C and 60°C water temperatures, respectively.
- The highest air side convection heat transfer coefficient ($h_{b,air}$) were obtained at 1646 and 1777 W/m²K for 50°C and 60°C water temperatures, respectively.
- The highest pressure drop measured at 14.16 l/s air flow rate was 3891 Pa.
- All three heat exchangers showed almost similar heat transfer characteristics. Type B showed slightly better heat transfer characteristics compared to the other 2 heat exchangers. This can be due to the pin walls added on the air manifolds to enhance air disturbance. However, further experiments are currently undergoing to define the best heat transfer characteristics.
- The pressure drop results indicate that modifying the air microchannel orientation has negligible impact on air side pressure drop. this is due to the fact that this type of heat exchanger results in significant pressure drop mainly because of the air manifold configuration which is blocked at the end and air microchannel orientations have marginal impact on the overall pressure drop.
- Overall, additive manufacturing was observed to be capable of fabricating metal heat exchangers with complex interior designs. The smallest length scale fabricated was 0.48 mm (thickness of the fins)

Future Work

- Continuing testing our system with our Type A, B, and C heat exchangers for different water flow rates between 0.016 l/s and 0.13 l/s and different air flow rates of 2.83 l/s and 14.16 l/s and two inlet water temperatures of 50C and 60C.
- Conducting cost analysis for different heat exchanger designs. the cost analysis compares the design complexity with manufacturing cost. In addition it compares the additive manufacturing cost with conventional manufacturing techniques
- Improving heat exchanger design based on topology optimization techniques [2].
- In addition uncertainty analysis will be added in the future to help identify the superior heat exchanger design.

Acknowledgement

Western New England University is gratefully acknowledged for providing the financial support to complete this study. The authors also would like to thank Dave Follette from Advanced Digital Design and Fabrication (AddFab) at the University of Massachusetts, Amherst for additively manufacturing the heat exchanger.[3]

References

1. M. A. Arie, A. H. Shooshtari, R. Tiwari, S. V. Dessiatoun, M. M. Ohadi, J. M. Pearce, Experimental characterization of heat transfer in an additively manufactured polymer heat exchanger, Applied Thermal Engineering 113 (2017) 575–584.
2. E Dede, S Joshi, F Zhou, Topology Optimization, Additive Layer Manufacturing, and Experimental Testing of an Air-Cooled Heat Sink, Journal of Mechanical Design, NOVEMBER 2015, Vol. 137 / 111702-1
3. AddFab, UMass Amherst. URL https://www.umass.edu/ials/addfab